IET Systems Biology

Research Article

IET Journals
The Institution of Engineering and Technology

Parameter estimation of a meal glucose–insulin model for TIDM patients from therapy historical data

ISSN 1751-8849
Received on 1st June 2018
Revised 29th August 2018
Accepted on 5th September 2018
E-First on 14th November 2018
doi: 10.1049/iet-syb.2018.5038
www.ietdl.org

Oscar D. Sánchez[1], Eduardo Ruiz-Velázquez[1] ✉, Alma Y. Alanís[1], Griselda Quiroz[2], Luis Torres-Treviño[2]

[1]CUCEI, Universidad de Guadalajara, Av. Revolución 1500, Col. Universitaria, 44430 Guadalajara, Jal., México

[2]FIME, Universidad Autónoma de Nuevo León, Av. Universidad S/N, Ciudad Universitaria, 66455 San Nicolás de los Garza, Nuevo León, N.L., México

✉ *E-mail: eduardo.ruiz@cucei.udg.mx*

Abstract: The effect of meal on blood glucose concentration is a key issue in diabetes mellitus because its estimation could be very useful in therapy decisions. In the case of type 1 diabetes mellitus (T1DM), the therapy based on automatic insulin delivery requires a closed-loop control system to maintain euglycaemia even in the postprandial state. Thus, the mathematical modelling of glucose metabolism is relevant to predict the metabolic state of a patient. Moreover, the eating habits are characteristic of each person, so it is of interest that the mathematical models of meal intake allow to personalise the glycaemic state of the patient using therapy historical data, that is, daily measurements of glucose and records of carbohydrate intake and insulin supply. Thus, here, a model of glucose metabolism that includes the effects of meal is analysed in order to establish criteria for data-based personalisation. The analysis includes the sensitivity and identifiability of the parameters, and the parameter estimation problem was resolved via two algorithms: particle swarm optimisation and evonorm. The results show that the mathematical model can be a useful tool to estimate the glycaemic status of a patient and personalise it according to her/his historical data.

1 Introduction

Diabetes mellitus (DM) is a metabolic disorder in which levels of blood glucose are increased (hyperglycaemia); it could be caused by a defect in the secretion or action of a hormone called insulin. This hormone is produced by the pancreas; it is essential in the metabolism and one of its functions is to control levels of blood glucose. DM is a critical public health problem; it has been considered a global threat and one of the leading causes of death by the World Health Organization. In 2014, it was estimated that 422 million adults were living with DM; and, just in 2012, it caused 1.5 million deaths worldwide [1].

A particular type of DM is presented when the hormone insulin is not produced by the pancreas; it is called type 1 diabetes mellitus (T1DM) and its treatment consists in exogenous injections of insulin to regulate glycaemic values. However, T1DM is difficult to control due to the complexity of the dynamics of glucose and insulin in the body and its disturbances such as feeding, stress, or exercise [2]. To improve the treatment, an automatic glucose control for patients with T1DM has been, for a long time, an objective. This closed-loop system to automate insulin infusion could be accomplished by a continuous glucose monitoring, an insulin pump, and a control algorithm [3–7].

To achieve the goal of connecting the insulin pump and the glucose monitoring system with a control algorithm, a dynamic model of glucose–insulin is necessary [8]. Applications of the models, among others, can be, for example, to verify the effectiveness of a control scheme before clinical trials, this is, performed in silico assessment. In the literature, different types of glucose–insulin models have been reported, among them, we can cite [9–12]. On the other hand, there are approaches that not only consider the systematic response of glucose metabolism but also physiological aspects [13, 14]. Adopting some features of various models, Sorensen [15] raises the idea of having a compartment model to represent the major organs that interact in glucose–insulin dynamics. These organs are: the brain, heart, lungs, intestine, liver, kidney, and periphery. The mass balance analysis was performed in each of these compartments, and the result was a model formed by 19 non-linear differential equations, besides that it has been used successfully in control tasks. Among the most recent models, the model proposed by Dalla Man *et al.* [16] is worthy of mention. It is a model of the glucose–insulin system (GIS) describing the physiological behaviour of a human after food intake and through six compartments: glucose system, insulin system, gastrointestinal tract, muscle and adipose tissue, liver, and β-cell; it is accepted as one of the most realistic models. Based on the previous model, it was developed in the simulator UVA/Padova to represent different scenarios of T1DM [17].

On the other hand, a critical issue of physiological models is the set of parameters, both single-subject models and a nominal model describing a study population [18]. In many situations, the states of physiological systems are not fully measurable. Therefore, the problem of parameter estimation becomes an interesting task [18]. The measurements are approximated by directly characterising the system through measurable system states and outputs. The task of parameter estimation in physiological models for T1DM has been performed to represent different scenarios of this disease, such as the work presented in [19]; in there they build on a non-linear physiologically motivated time-varying model of glucose regulation. They adopted the Bayesian approach to estimate model parameters and to obtain the posterior probability distribution of time-invariant and time-varying parameters through the use of Markov chain via Monte Carlo methodology. This was carried out in the model of Hovorka [19]. A similar work was performed in [20], they propose a Bayesian method for the identification of a model from plasma glucose and insulin concentrations, by exploiting the prior model parameter distribution; five parameters of the UVA/Padova model were identified by this method. Recently, Biswas *et al.* proposed the estimation of some biological parameters in DM patients using only glucose measurements. Virtual patient measurements generated with Matlab software are combined with glucose–insulin homeostasis model with a Bayesian non-linear filter used as estimator [21]. Most parameter estimation schemes consider parameters invariant in time, but it has been observed that the dynamics of glucose–insulin changes throughout the day and from one day to the next, which suggests that some parameters change over the time [22, 23].

Parameter estimation is not a trivial task; often, the models contain several ordinary differential equations and numerous parameters that make difficult to use traditional methods to estimate parameters. Currently, a wide range of analytical techniques exists for linear systems [24]. For non-linear systems, limited progress has been made with those methods. On the other hand, some success has been achieved with traditional optimisation algorithms. The principal problem with conventional techniques is their dependence on unrealistic assumptions such as unimodal landscapes and differentiability and continuity of the objective function [25]. As a result, non-linear problems are oversimplified to fulfil such assumptions.

Evolutionary algorithms (EAs) are a promising alternative to traditional approaches. Since EA does not depend on assumptions such as unimodality, differentiability, or continuity. They are capable of handling problems with non-linear constraints, multiple objectives, and time-varying components. In addition, they have shown superior performance in numerous real-world applications [25]. Such as the one used in parameter estimation of biological models in [26], in which a differential EA is used to estimate the unknown parameters of a gene regulatory network model.

In this work, we focus on the use of EA to solve the parameter estimation problem of a meal glucose–insulin model for a T1DM patient. The objective is to capture the non-linear behaviour of the blood glucose metabolism through a meal glucose–insulin model approach. The following problems are approached in this paper: (i) sensitivity analysis and identifiability analysis of the Dalla Man model; (ii) parameter estimation using EA; (iii) establish a set of time-varying parameters. Solving these three problems, the paper is organised as follows: first, the Dalla Man model is presented; then the sensitivity and identifiability of the model are analysed. After that, two EAs to resolve the parameter estimation are described; and finally, the results and conclusion are presented.

2 Model

The Dalla Man model is a compartmental model based on the principle of matter conservation from which a system of differential equations is obtained to represent glucose–insulin in organs and tissues [16]. The model is composed of six compartments: gastrointestinal tract, liver, glucose system, muscle and adipose tissue, β-cell, and insulin system. In order to use the model as one of the T1DM, the β-cell compartment is removed and replaced by the subcutaneous insulin infusion model. In addition, the dynamics of the CMGS sensor is added.

Subcutaneous insulin infusion module: This model is used to describe the appearance rate of insulin in plasma when there are exogenous infusions [27].

Continuous glucose monitoring model: This model is added to use historical data collected from a glucose sensor. Only a differential equation is employed to describe the delay between blood glucose and the measurement of the glucose sensor. Thus, the model is expressed by a linear differential equation [28].

2.1 Affine system

In order to study the Dalla Man's set equations in [16, 27], it could be represented in an affine system manner. It is through a set of ordinary differential equations of the form

$$\Sigma\begin{cases}\dot{\boldsymbol{x}} = f(\boldsymbol{x},\boldsymbol{p}) + g(\boldsymbol{x},\boldsymbol{p})\boldsymbol{u}\\ \boldsymbol{y} = h(\boldsymbol{x})\end{cases} \tag{1}$$

where $\boldsymbol{x} = \{\boldsymbol{x}_1, \ldots, \boldsymbol{x}_n\} \in \mathbb{R}^n$ is the state variable, $\boldsymbol{p} = \{p_1, \ldots, p_q\} \in \mathbb{R}^q$ the unknown/uncertain parameter vector in parameter space P, $\boldsymbol{u} = \{u_1, \ldots, u_{n_u}\} \in \mathbb{R}^{n_u}$ the input (control) vector, $\boldsymbol{y} = \{\boldsymbol{y}_1, \ldots, \boldsymbol{y}_m\} \in \mathbb{R}^m$ the m -dimensional output. $f(\boldsymbol{x},\boldsymbol{p})$ is a smooth non-linear function. The state equation of the model can be written as

$$\begin{aligned}
\dot{\boldsymbol{x}}_1 &= k_{p1} - F_{\text{cns}} - k_1\boldsymbol{x}_1 + k_2\boldsymbol{x}_2 - k_{p2}\boldsymbol{x}_1 - k_{p3}\boldsymbol{x}_6\\
&\quad + k_{e1}(k_{e2} - \boldsymbol{x}_1) + \frac{(fk_{\text{abs}}\boldsymbol{x}_9)}{BW}\\
\dot{\boldsymbol{x}}_2 &= k_1\boldsymbol{x}_1 - k_2\boldsymbol{x}_2 - \frac{(\boldsymbol{x}_2(V_{m0} + V_{mx}\boldsymbol{x}_{10}))}{(K_{m0} + \boldsymbol{x}_2 + K_{mx}\boldsymbol{x}_{10})}\\
\dot{\boldsymbol{x}}_3 &= m_2\boldsymbol{x}_4 - \boldsymbol{x}_3\left(m_1 - \frac{(m_1m_6)}{(m_6 - 1)}\right)\\
\dot{\boldsymbol{x}}_4 &= k_{a1}\boldsymbol{x}_{11} - \boldsymbol{x}_4(m_2 + m_4) + k_{a2}\boldsymbol{x}_{12} + m_1\boldsymbol{x}_3\\
\dot{\boldsymbol{x}}_5 &= -k_i\left(\boldsymbol{x}_5 - \frac{\boldsymbol{x}_4}{V_I}\right)\\
\dot{\boldsymbol{x}}_6 &= k_i(\boldsymbol{x}_5 - \boldsymbol{x}_6)\\
\dot{\boldsymbol{x}}_7 &= -k_{\text{gri}}\boldsymbol{x}_7 + D(t)\delta(t)\\
\dot{\boldsymbol{x}}_8 &= k_{\text{gri}}\boldsymbol{x}_7 - \boldsymbol{x}_8\left(k_{\min} + \left(\frac{k_{\max}}{2} - \frac{k_{\min}}{2}\right)\right.\\
&\quad \times (\tanh(a(\boldsymbol{x}_7 + \boldsymbol{x}_8 - bD(t)))\\
&\quad \left. -\tanh(c(\boldsymbol{x}_7 + \boldsymbol{x}_8 - dD(t))) + 2)\right)\\
\dot{\boldsymbol{x}}_9 &= \boldsymbol{x}_8\left(k_{\min} + \left(\frac{k_{\max}}{2} - \frac{k_{\min}}{2}\right)\right.\\
&\quad \times (\tanh(a(\boldsymbol{x}_7 + \boldsymbol{x}_8 - bD(t)))\\
&\quad \left. -\tanh(c(\boldsymbol{x}_7 + \boldsymbol{x}_8 - dD(t))) + 2)\right) - k_{\text{abs}}\boldsymbol{x}_9\\
\dot{\boldsymbol{x}}_{10} &= -p_{2U}\left(I_b - \frac{\boldsymbol{x}_4}{V_I}\right) - p_{2U}\boldsymbol{x}_{10}\\
\dot{\boldsymbol{x}}_{11} &= \boldsymbol{u} - \boldsymbol{x}_{11}(k_{a1} + k_d)\\
\dot{\boldsymbol{x}}_{12} &= k_d\boldsymbol{x}_{11} - k_{a2}\boldsymbol{x}_{12}
\end{aligned} \tag{2}$$

where $\boldsymbol{x}_1 = G_p$, $\boldsymbol{x}_2 = G_t$, $\boldsymbol{x}_3 = I_l$, $\boldsymbol{x}_4 = I_p$, $\boldsymbol{x}_5 = I_1$, $\boldsymbol{x}_6 = I_d$, $\boldsymbol{x}_7 = Q_{\text{sto1}}$, $\boldsymbol{x}_8 = Q_{\text{sto2}}$, $\boldsymbol{x}_9 = Q_{\text{gut}}$, $\boldsymbol{x}_{10} = X$, $\boldsymbol{x}_{11} = I_{\text{sc1}}$, $\boldsymbol{x}_{12} = I_{\text{sc2}}$, $\boldsymbol{y} = G$, $\boldsymbol{u} = IIR$.

3 Analysis of the model

3.1 Equilibrium point

Both the concentration of glucose and insulin are discussed in terms of the solution of (2) for T1DM model. If it exists, the equilibrium point $\boldsymbol{x}^* \in \mathbb{D}$ satisfies $f(\boldsymbol{x}^*, \boldsymbol{p}) = 0$ and is a solution such that the application $f: \mathbb{D} \to \mathbb{R}^{12}$ maps the point $\boldsymbol{x}^*$ into the point 0. That is, concerning to the GIS, the point $\boldsymbol{x}^*$ cancels the dynamics $\dot{\boldsymbol{x}}$ and can represent the basal BGL. The equilibrium point for nominal values of parameters is given by $f(\boldsymbol{x},\boldsymbol{p}) = 0$

$$\boldsymbol{x}^* = [264 \quad 202 \quad 0 \quad 0 \quad 0 \quad 0 \quad 0 \quad 0 \quad 0 \quad 0 \quad 0 \quad 0]^{\text{T}} \tag{3}$$

3.2 Sensitivity analysis

The parametric sensitivity analysis defines how sensitive is the solution of a dynamical system in relation to changes in its parameters. From biomedical sciences point of view, parametric sensitivity is reported in a normalised form to compare phenomena [29]. In the problem of parametric identification, this analysis helps to reduce the number of parameters to be identified. From dynamical systems and control theory, the effect of parameter variations can be captured in the frequency response of a dynamical system [30]. Frequency response permits to capture the effect onto a controlled variable due to parametric uncertainty [30]. The parametric sensitivity analysis permits additionally to find what parameters have effect on the time evolution of the concentrations as well as the basal level.

Since the equilibrium $\boldsymbol{x}^*$ is a solution of the system, the effects of the parameters entail a modification on its coordinates as well. By nature, the parameters are important in the production and uptake glucose. Thus, the parameters have been selected such that the parameters affect the solutions of (1) in a more sensitive way. The algorithm used for sensitivity analysis has been taken from [31]. The underlying idea is to define a sensitivity function, namely S, involving two matrices. One of them is the Jacobian matrix with

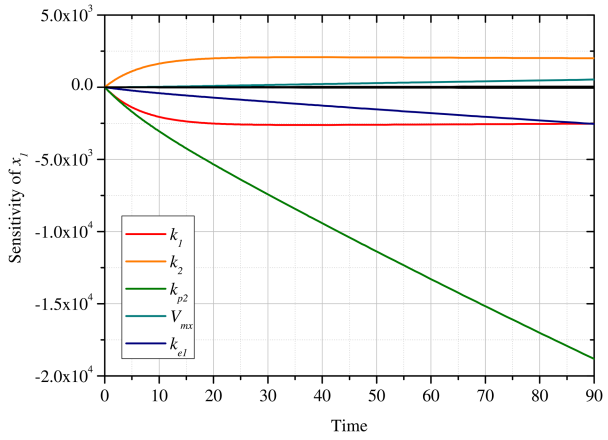

Fig. 1 *Glucose masses in plasma and rapidly equilibrating tissues ($\boldsymbol{x}_1$) are mostly sensitive to parameters k_1, k_{p2}, k_2, k_{e1}, and V_{mx}*

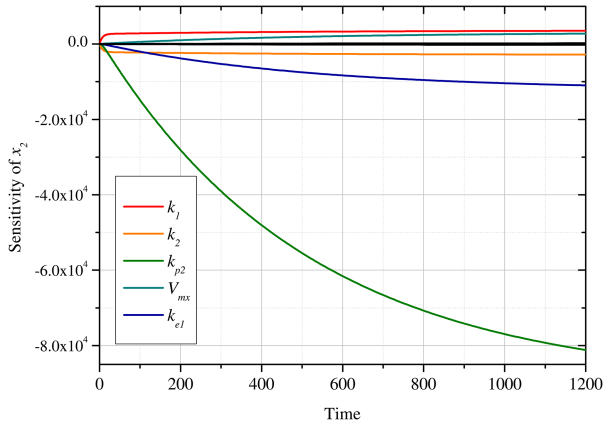

Fig. 2 *Glucose masses in plasma and slowly equilibrating tissues ($\boldsymbol{x}_2$) are mostly sensitive to parameters k_1, k_{p2}, k_2, k_{e1}, and V_{mx}*

Table 1 Values of sensitive parameters for $\boldsymbol{x}_1$ (first line) and $\boldsymbol{x}_2$ (second line)

Sensitive parameters	Magnitude
$k_1, k_{p2}, k_2, k_{e1}, V_{mx}$	−2500, −11× 10^4, 350, −1200, 2000
$k_1, k_{p2}, k_2, k_{e1}, V_{mx}$	3000, −9× 10^4, −2700, −1.1× 10^4, 1500

respect to states $\boldsymbol{x} \in \mathbb{D}$ evaluated in $\boldsymbol{x}^* \in \mathbb{D}$. The entries of the latter are given by the partial derivative of the vector field with respect to the parameters $\boldsymbol{p} \in P$ evaluated at the nominal values $p_0 \in P$, $A(\boldsymbol{x}, \boldsymbol{p}) = [(\partial f(t, \boldsymbol{x}, \boldsymbol{p}))/\partial \boldsymbol{x}]|_{x^*}$ and $B(\boldsymbol{x}, \boldsymbol{p}) = [(\partial f(t, \boldsymbol{x}, \boldsymbol{p}))/\partial \boldsymbol{p}]|_{p_0}$. Then the sensitivity function becomes

$$\dot{S} = A(\boldsymbol{x}, \boldsymbol{p})s + B(\boldsymbol{x}, \boldsymbol{p}) \tag{4}$$

where $\boldsymbol{S} = \boldsymbol{x}_p(t, p_0)$. $\boldsymbol{S} = [\partial \boldsymbol{x}/\partial p]\big|_{p_0} \in \mathbb{R}^{12\times 27}$ is a matrix whose entries are the state variation concerned to each parameters. Henceforth, $S(t) \in \mathbb{R}^{12\times 27} \times \mathbb{R}$ provides the sensitivity of the state $\boldsymbol{x} \in \mathbb{D}$ with respect to the parameters $\boldsymbol{p} \in H$ along time $t \in \mathbb{R}$. The sensitivity of the glucose subsystem in the Dalla Man model is shown in Figs. 1 and 2.

Table 1 is a summary of the sensibility analysis; it presents the most sensitivity parameters for $\boldsymbol{x}_1$ and $\boldsymbol{x}_2$, which are the states that describe the glucose kinetics. The magnitude indicates that how much is the sensibility of the response in the state due to the variation of the parameter, also if the parameter should be increased or decreased.

This result is a criterion to choose the parameters that have a greater relevance in the solution of the system (2). In addition, it helps to not estimate those parameters that are practically constant because their variation does not affect the solution of the system, especially plasmatic glucose.

3.3 Structural identifiability analysis

Another analysis necessary for identification is the identifiability, that is, the ability to identify the parameters of a dynamical system through its input–output behaviour. The identifiability property is a prerequisite to resolve a parameter estimation problem; it guarantees that parameters in a dynamical system can be determined from measured data [32].

In accordance with the methodology used in [33], the problem of parametric identifiability can be treated as a case of observability problem. Under some consideration, a parameter is treated as a state variable with time derivative zero, i.e. $\dot{p} = 0$; thus, the observability rank test is used to determine parameter identifiability. For a non-linear system (1) with $\dot{p} = 0$ for the analysis, $\boldsymbol{x}$ and $\boldsymbol{p}$ are considered as the same type of variables. Without initial conditions for $\boldsymbol{x}$, the non-observable variables can be both in $\boldsymbol{x}$ and $\boldsymbol{p}$. Considering a full set of initial conditions on $\boldsymbol{x}$, i.e. $\boldsymbol{x}(0) = \boldsymbol{x}^0$. Then the problem of observability of the $\boldsymbol{x}$ variables disappears [32]. For the analytical system (1), the rank test gives the rank of the following Jacobian

$$O_N = \begin{bmatrix} \dfrac{\partial h(\boldsymbol{x})}{\partial \boldsymbol{p}} \\ \dfrac{\partial L_f h(\boldsymbol{x})}{\partial \boldsymbol{p}} \\ \vdots \\ \dfrac{\partial L_f^{n-1} h(\boldsymbol{x})}{\partial \boldsymbol{p}} \end{bmatrix} \tag{5}$$

where $L_f h = \dfrac{\partial h(\boldsymbol{x})}{\partial \boldsymbol{x}} f(\boldsymbol{x}, \boldsymbol{p})$ is the Lie derivative [33]. Then, (5) is locally identifiable if

$$\operatorname{rank}(O_N(\boldsymbol{p})) = q \tag{6}$$

Consider $p^* \in P$ and note that for all $\boldsymbol{p}$ in the neighbourhood of p^*(i.e. $\boldsymbol{p} \in V(p^*)$)

$$\boldsymbol{y} = O_N(\boldsymbol{p})\boldsymbol{p} \tag{7}$$

Then, condition (6) implies that for $\boldsymbol{p} \in V(p^*)$

$$\boldsymbol{p} = \left(O_N(\boldsymbol{p})^{\mathrm{T}} O_N(\boldsymbol{p})\right)^{-1} O_N(\boldsymbol{p})^{\mathrm{T}} \boldsymbol{y} \tag{8}$$

In addition, identifiability tableau is a way to check the structural identifiability problems and to help in the solution of the non-linear system [34]. It shows the non-zero elements of the Jacobian of the series coefficients with respect to the parameters. It is a table with the same numbers as columns as parameters and as many rows as non-zero series coefficients. If the rank of the Jacobian coincides with the number of parameters, then the parameters will be locally identifiable (which implies that the parameter or parameters can be estimated). On the other hand, the rank is deficient, when empty rows appear (this corresponds to non-identifiable parameter), or if the number of Lie derivatives is insufficient.

In the case of a row with only a non-zero element appears in the tableau, then the corresponding parameter is structurally identifiable. These rows are eliminated, then it is generated a reduced tableau, which leads to the appearance of new unique non-zero elements.

3.4 Implementation of the method

In this work, we used the software GenSSI [35] to find structural identifiability. This software is based upon the generating series approach coupled to the use of identifiability tableaus [34].

The test was performed for 27 parameters of the Dalla Man model. The body weight parameter was discarded because it is considered invariant in a person. Fig. 3 shows the reduced identifiability tableau of order one, which represents the non-zeros columns with respect to each parameter used in the analysis. After

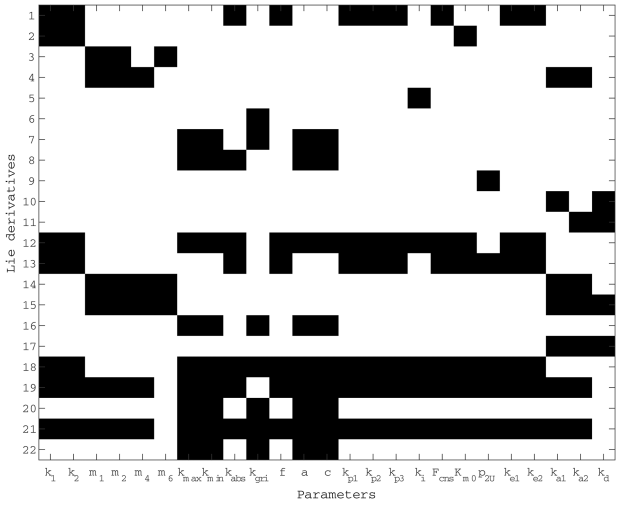

Fig. 3 *Reduced identifiability tableau of order one. The rows are associated with the corresponding Lie derivatives components, whereas the columns are associated with the corresponding parameter*

eliminating the columns of parameters structurally identifiable and those parameters structurally non-identifiable, the order one tableau becomes full rank. From the identifiability analysis, the parameters b and c resulted structurally non-identifiable, for this reason, they were discarded in the solution of the parameter estimation problem. The remaining parameters used in the test resulted in at least structurally locally identifiable. Therefore, we can say it is possible to estimate them.

4 Solving parameter estimation via EA

4.1 Evonorm

The EA Evonorm proposed by Torres-Treviño [36] replaced the crossover and mutation mechanisms by a distribution function. The iterative process of Evonorm algorithm is described by:

i. evaluation of a population P;
ii. selection of the best individuals $\boldsymbol{P}_{\mathrm{S}}$ from P;
iii. generation of a new population P using the best individuals $\boldsymbol{P}_{\mathrm{S}}$.

A population P is generated through a matrix of size $I_p \times D_r$, where I_p is total of individuals and D_r the total of possible decision variables. A potential solution is represented as an individual and is given by each row of P. This algorithm has a deterministic selection mechanism to determine the fittest individuals. The chosen individuals form a matrix $\boldsymbol{P}_{\mathrm{S}}$ of size $I_s \times D_r$, where I_s is the total of chosen individuals. Always, the number of selected individuals I_s is lower than the number of original population I_p, usually, it is used around of 10–20% of total population. Then to generate a new population, the mean μ_{pr} and standard deviation σ_{pr} are computed using the total of the chosen individuals, this is

$$\mu_{pr} = \frac{1}{I_s}\sum_{k=1}^{I_s} \boldsymbol{P}_{S_{k,\,pr}} \tag{9}$$

$$\sigma_{pr} = \sqrt{\frac{1}{I_s}\sum_{k=1}^{I_s} \left(\boldsymbol{P}_{S_{k,\,pr}} - \mu_{pr}\right)} \tag{10}$$

where $pr \in \{1; 2; 3; \ldots; D_{rg}\}$, the mean μ_{pr} and σ_{pr} for the D_r decision variables are used for a normal random variable to generate a new population P. The stochastic process is combined with a heuristic to maintain the equilibrium between exploration and exploitation. Then, new solutions can be found not necessary near to the mean. The individuals $P_{i,\,pr}$ of a new population $\boldsymbol{P}$ are obtained using the best solution $I_{\boldsymbol{x}_{pr}}$ founded in each generation that is involved in the new population for the 50 % of times, and in the other case, the mean μ_{pr} is used

$$P_{i,\,pr} = \begin{cases} N(\mu_{pr}, \sigma_{pr}) & U(\bullet) > 0.5 \\ N\left(I_{\boldsymbol{x}_{pr}}, \sigma_{pr}\right) & \text{otherwise} \end{cases} \tag{11}$$

The variable $U(\bullet)$ has a uniform distribution function; $N(\bullet)$ is a random variable with a normal distribution function.

4.2 Particle swarm optimisation

Particle swarm optimisation (PSO) is an EA that generates a population based on stochastic optimisation technique proposed by Kennedy and Eberhart [37, 38]. The concept of PSO is based on the social interaction behaviour of birds flocking and fish schooling. For simulation, the PSO initialises a population of particles randomly positioned in an n-dimensional search space. Each particle in the population has two vectors, a velocity vector and a position vector. Each particle is updated through its velocity and position vectors by learning from its historically position, and the best position found by the total swarm for each generation. Let $\boldsymbol{V}_i(v_i^1, v_i^2, \ldots, v_i^n)$ and $\boldsymbol{X}_i(\boldsymbol{x}_i^1, \boldsymbol{x}_i^2, \ldots, \boldsymbol{x}_i^n)$, where the ith particle is the velocity vector and position vector, respectively, and M is the total of particles in a population. The PSO algorithm is given by the equations

$$v_i^j = wv_i^j + c_1\mathrm{rand}_1\left(p\mathrm{Best}_i^j - \boldsymbol{x}_i^j\right) + c_2\mathrm{rand}_2\left(g\mathrm{Best}_i^j - \boldsymbol{x}_i^j\right) \tag{12}$$

$$\boldsymbol{x}_i^j = \boldsymbol{x}_i^j + v_i^j \tag{13}$$

where $p\mathrm{Best}_i = \left(p\mathrm{Best}_i^1, p\mathrm{Best}_i^2, \ldots, p\mathrm{Best}_i^n\right)$ are the best positions of particle $i = (1, 2, \ldots, M)$, then the best positions by the swarm is $g\mathrm{Best} = \left(g\mathrm{Best}^1, g\mathrm{Best}^2, \ldots, g\mathrm{Best}^n\right)$, w is the inertia factor, c_1 and c_2 are parameters to weigh the relative importance of $p\mathrm{Best}_i$ and $g\mathrm{Best}$; respectively. rand_1 and rand_2 are any numbers generated random uniformly distributed into $[0, 1]$, and $j = (1, 2, \ldots, n)$ represents the jth dimension of the search space. PSO is one of the most popular optimisation techniques because it has been successfully applied in different areas, e.g. [39–42].

5 Results

5.1 Experimental data

The experimental historical data used to solve the identification of the Dalla Man model are collected from two diabetic women, the first one is, 23 years old, 14 years since T1DM diagnosis, 1.68 m, 58.5 kg; the second one is 27 years old, 12 years since T1DM diagnosis, 1.62 m, 56 kg. The patients did not present any other complication or disease associated with DM. Collected data were selected 2 days and half from a total historical data, under medical supervision and standard ingest (three meals and some snacks) and without exercise events.

Experimental blood glucose data was obtained using paradigm real-time insulin pump and continuous glucose monitoring system (CGMS) by MiniMed Inc. The insulin pump was used for the T1DM treatment, it delivers preprogrammed basal rates and preprandial bolus subcutaneously. The patient updates the information based on her particular condition, such that blood glucose level was maintained in the euglycaemic range. Also, the patient had to provide to insulin pump the quantity of carbohydrates for each meal. Glucose sensor was connected to patient subcutaneously, which provides a sample of interstitial blood glucose in a sample of time of 5 min to CGMS included in the insulin pump. When the lifetime of the sensor is over, the experimental data with blood glucose concentration, subcutaneous insulin infused, and grams of carbohydrate in meals can be stored in a computer. The data provided by this technological system were used to obtain the dynamic behavioural of glucose–insulin and carbohydrate. Then, the recollected data were

i. The records of sensor glucose (SG(t)) through 60 h (one value every 5 min).
ii. The infused insulin was recollected of the insulin injected to the patient (one value every 1 min).
iii. The carbohydrate ingest provided by the patient.

In order to simulate the proposed physiological model, D and $U(t)$ are considered as the system input. D represents the total carbohydrates ingested at each meal, and $U(t)$ is the insulin delivered at the subcutaneous route through an insulin pump. $\boldsymbol{y} = \mathrm{SG}(t)$ is the output system representing the glucose obtained by the sensor. Figs. 4 and 5 display the input signals considered as the carbohydrate consumption (top), the insulin concentration after absorption (middle), and the records from CGMS (bottom).

5.2 Estimation results

The previous data set was used to perform parametric estimation. From the total parameters, only 11 were selected considering the sensibility analysis, identifiability analysis, and due to the complexity of the dynamic of the DMT1. From the sensibility analysis, the parameters k_1, k_2, k_{p2}, k_{e1}, and k_{p1} were selected. In addition from the work in [20], the parameters $k_{\max}$, $k_{\min}$, k_{abs}, k_{p3}, and k_{gri} were selected. Also, a time window is defined to estimate the parameters for the model. For every time window, five samples were considered or intervals of 25 min. Fig. 6 represents the methodology to resolve the parameter identification problem and it can be summarised in the following six steps (using any of the two algorithms). The steps for parametric identification for the two algorithms (PSO and Evonorm) were:

i. Initialise the interval $[t_{\mathrm{i}},\ t_{\mathrm{f}}]$, where $t_{\mathrm{i}} = 1$ and $t_{\mathrm{f}} = 5$.
ii. Extract a time window from t_{i} to t_{f} from the historic data glucose X_{D}, insulin U_{D}, and carbohydrates D_{D}.
iii. Parameters to be estimated $\boldsymbol{p} = [k_{p2}\ \ k_1\ \ k_2\ \ k_{p1}\ \ k_i\ \ k_{e1}\ \ k_{\max}\ \ k_{\min}\ \ k_{\mathrm{abs}}\ \ k_{p3}\ \ k_{\mathrm{gri}}]$.
iv. Solve the Dalla Man model (2) and CGMS model [28] in the initial time t_{i} until the final time t_{f} using the inputs of the system $\boldsymbol{u} = [U_{\mathrm{D}} D_{\mathrm{D}}]$. The solution on the time window is extract of $\boldsymbol{y} = \mathrm{SG}(t)$, because it represents the glucose sensor levels (see Section 2).
v. Compute fitness error using

$$f_{\mathrm{error}} = \frac{1}{n}\sum_{m=t_{\mathrm{i}}}^{t_{\mathrm{f}}} \sqrt{(\log(\mathrm{SG}(m)) - \log(X_{\mathrm{D}}(m)))^2} \qquad (14)$$

where n represents the total data used for evaluation in the time window (m) from t_{i} to t_{f}. SG(m) represents the sensor glucose concentration in every time m. $X_{\mathrm{D}}(m)$ stores the real sensor glucose on time m.
vi. If the error cannot be reduced any more, go to the next step, else back to step iii.
vii The time window is updated: $t_{\mathrm{i}} \leftarrow t_{\mathrm{i}} + 5$, $t_{\mathrm{f}} \leftarrow t_{\mathrm{f}} + 5$.
.
vii If there are more data in the next time window, go to step ii,
i. else end.

The numerical experiments were performed to estimate the sensor glucose SG, from the parameter sets computed by the EA algorithms Evonorm and PSO. The experiment with each algorithm is depicted in Fig. 7 for Evonorm and Fig. 8 for PSO. The estimated PSO data and Evonorm data are represented by a blue line, and the real data is shown by a red line. The estimation error $e(m)$ (Figs. 9 and 10) for Evonorm and PSO is defined as the subtraction of the measured data $X_{\mathrm{D}}(M)$ and the estimated one SG(M) at the complete interval $M = 1; \ldots; 704$.

The results show that PSO has a better behaviour than Evonorm. Table 2 shows that the mean square error achieved by Evonorm is 5.35584 mg/dl with a standard deviation of 3.11611 mg/dl for the first patient; and 8.74460 mg/dl with a standard deviation of 5.62151 mg/dl for the second patient. PSO has a good performance too, with a mean square error of 4.08388 mg/dl, a standard deviation of 2.48674 mg/dl for the first patient, and 6.99935 mg/dl with a standard deviation of 4.63225 mg/dl for the second patient. Considering the information provided to the system, the results are acceptable. Thus, resolving the parameter estimation problem, the model gives a response close to the data provided by the patients.

Tables 3 and 4 show the mean and the standard deviation of the estimated parameters obtained by Evonorm and PSO, respectively. It can be seen that both algorithms found similar values of the

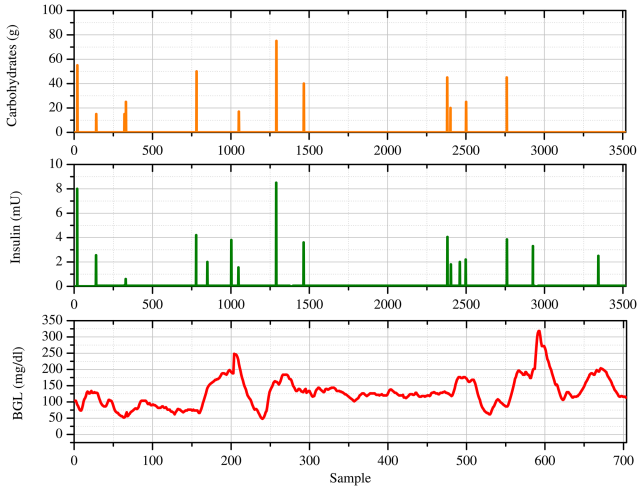

Fig. 4 *Patient number 1 historical data: carbohydrate consumption (top), insulin infusion (middle), glucose concentration (bottom)*

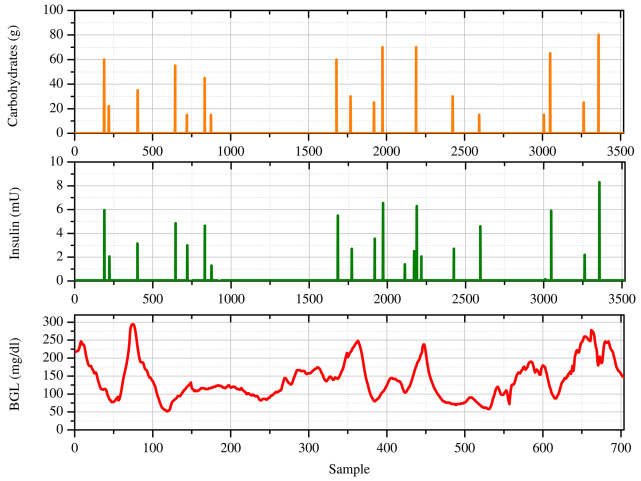

Fig. 5 *Historical recollected data of patient number 2: carbohydrate consumption (top), insulin infusion (middle), glucose concentration (bottom)*

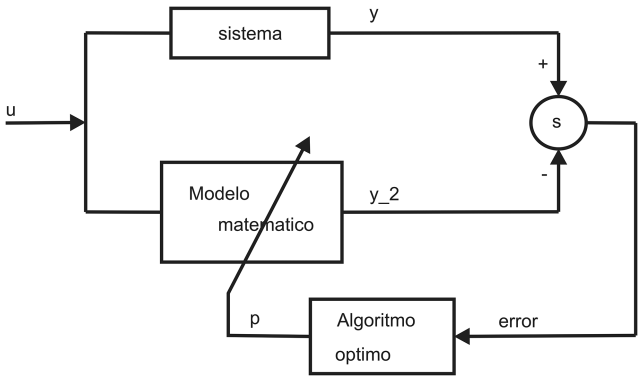

Fig. 6 *Representative diagram to resolve the parameter estimation problem using an EA (optimiser algorithm)*

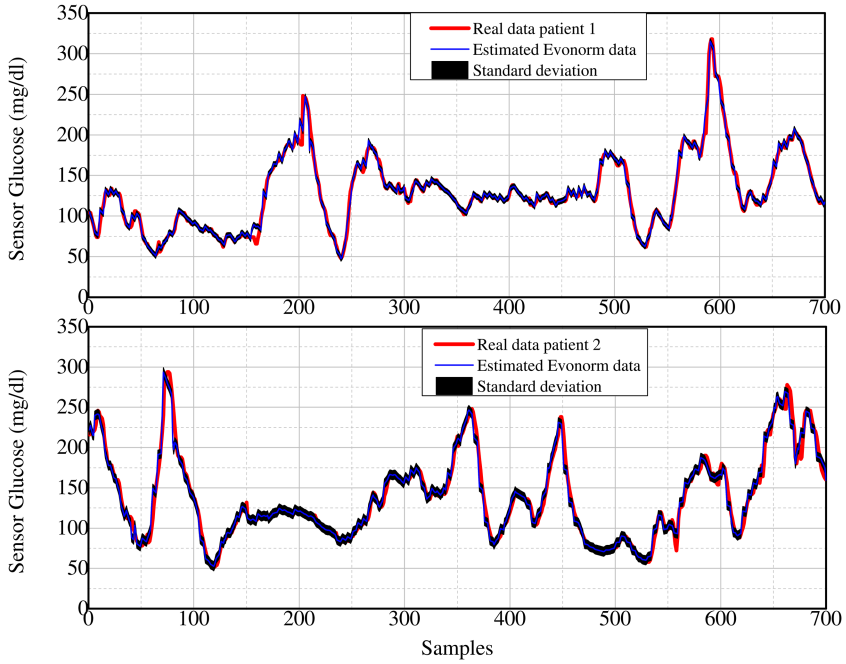

Fig. 7 *Blood glucose concentration of patients estimated by Evonorm algorithm*

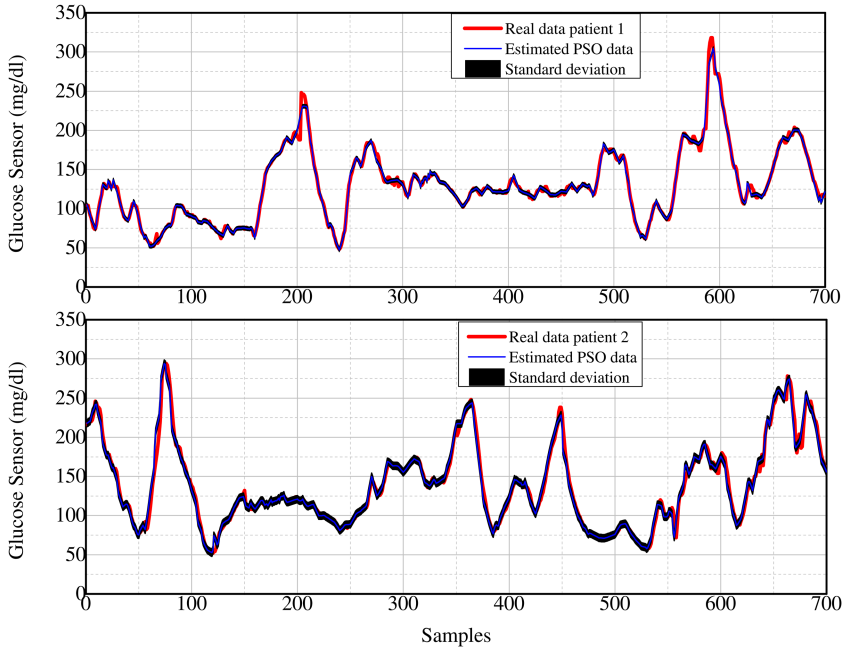

Fig. 8 *Blood glucose concentration of patients estimated by PSO algorithm*

parameters, and a similar range for each parameter. The range found for each parameter can be useful to represent different metabolic conditions of patients.

In order to analyse the behaviour of both EA presented in this work, the Wilcoxon sign-rank test was performed. This is a statistical technique that uses the fitness error of each time window in the following manner [42]. It is assumed n time windows from a data set with two observations $\boldsymbol{x}i$ and $\boldsymbol{y}i$ for each time window i. This results in two paired samples $\boldsymbol{x}_1, \ldots, \boldsymbol{x}_n$ and $\boldsymbol{y}_1, \ldots, \boldsymbol{y}_n$. Then *T-statistic* is the sum of the negative ranges obtained by $z_i = \boldsymbol{y}_i - \boldsymbol{x}_i$ for all $i = 1, \ldots, n$.

In this test, we use the following null hypothesis. H_0: the distribution of difference scores in two algorithms is symmetric at about zero. The critical values for the T statistic are evaluated in a normal distribution Z. Here, we use $\alpha = 0.5$ for Evonorm versus PSO for patient number 1 with $n = 141$, $\alpha = 0.5$. Since for Evonorm versus PSO, $Z = -3.1417 > 1.96 = Z_\alpha$, we cannot reject the null hypothesis, and we can conclude that there is not a significant difference between the two algorithms. For Evonorm versus PSO for patient number 2 with $n = 141$, $\alpha = 0.5$. Since for Evonorm versus PSO, $Z = -4.1110 > 1.96 = Z_\alpha$, then, we cannot reject the null hypothesis, and we can conclude that there is not a significant difference between the two algorithms. Hence, both algorithms have similar results; this means that none of the algorithms is better for this experiment. However, they have proven to be good to resolve the problem of parametric identification, even though the search space is large.

6 Conclusion

To represent the dynamics of T1DM is not an easy task and it may become more complicated to try to represent a population suffering with DMT1 through a single mathematical model with nominal parameters. In this work, we propose a methodology to identify a mathematical model resolving a parameter estimation problem via an analysis of sensitivity and identifiability of parameters. In this way, it is representative of the dynamics of meal glucose–insulin

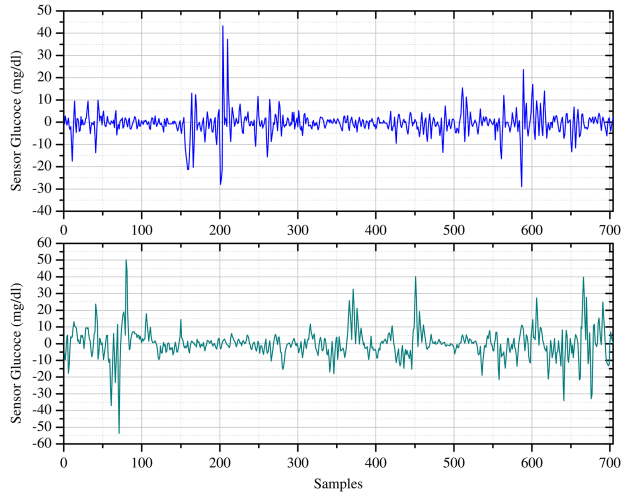

Fig. 9 *Estimation error of the measured data and the estimated data by Evonorm. Error of patient number 1 (top), error of patient number 2 (bottom)*

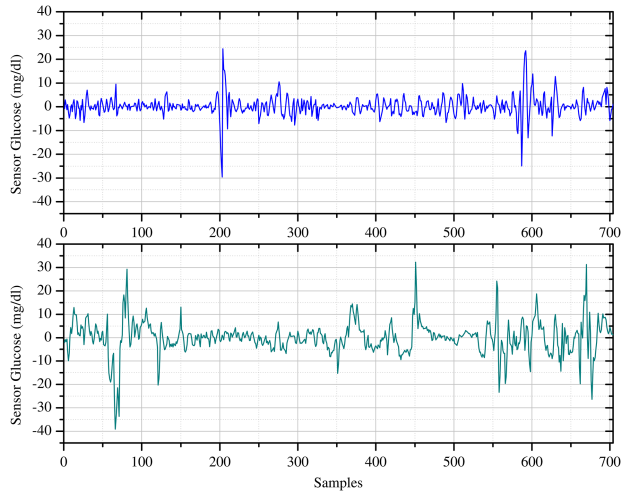

Fig. 10 *Estimation error of the measured data and the estimated data by PSO. Error of patient number 1 (top), error of patient number 2 (bottom)*

Table 2 Mean square error (MSE) and the standard deviation (SD) obtained by PSO and Evonorm algorithms

Patient	PSO		Evonorm	
	MSE (dl/mg)	SD (dl/mg)	MSE (dl/mg)	SD (dl/mg)
1	4.08388	2.48674	5.35584	3.11611
2	6.99935	4.63225	8.74460	5.62151

Table 3 Mean and the standard deviation (SD) of the parameters obtained by Evonorm

Parameter	Patient no. 1		Patient no. 2	
	Mean	SD	Mean	SD
k_{p2}	0.0963	±0.0645	0.0930	±0.0649
k_1	0.0430	±0.0326	0.0599	±0.0306
k_2	0.0432	±0.0330	0.0178	±0.0219
k_{p1}	2.1623	±1.3023	1.9307	±1.2198
k_i	0.0048	±0.0031	0.0053	±0.0033
k_{abs}	0.0412	±0.0333	0.0313	±0.0305
k_{e1}	0.0005	±0.0003	0.0005	±0.0003
k_{max}	0.0466	±0.0340	0.0526	±0.0346
k_{min}	0.0050	±0.0032	0.0047	±0.0031
k_{p3}	0.0051	±0.0033	0.0048	±0.0034
k_{gri}	0.0499	±0.0337	0.0475	±0.0324

Table 4 Mean and the standard deviation (SD) of the parameters obtained by PSO

Parameter	Patient no. 1		Patient no. 2	
	Mean	SD	Mean	SD
k_{p2}	0.0432	±0.0727	0.0493	±0.0777
k_1	0.0115	±0.0210	0.0172	±0.0268
k_2	0.0574	±0.0407	0.0473	±0.0413
k_{p1}	2.0675	±1.4474	2.1100	±1.5361
k_i	0.0048	±0.0044	0.0050	±0.0044
k_{abs}	0.0505	±0.0425	0.0529	±0.0426
k_{e1}	0.0005	±0.0004	0.0004	±0.0004
k_{max}	0.0504	±0.0431	0.0489	±0.0429
k_{min}	0.0476	±0.0436	0.0511	±0.0444
k_{p3}	0.0055	±0.0042	0.0045	±0.0044
k_{gri}	0.0477	±0.0446	0.0472	±0.0435

with parameters that vary over time; from the point of view of control, these parameters can be considered to be similar to uncertain parameters, which would help to find alternatives in the design of robust controllers that are close to real-time actuality. In this sense, the main contribution of this work is that the parameter estimation problem resolved via EA allows us to establish a set of parameters, and the range into they can evolve, such that the mathematical model can reproduce the dynamic of the metabolism of a single patient via her historical data. The results obtained by Evonorm algorithm are close to the T1DM patient historical real data with an acceptable error; also, PSO algorithm had good results in solving the parameter estimation problem. As future work, an individual T1DM patient model can be designed according to the requirements to implement online algorithms of parameter estimation, control algorithms as adaptive schemes or simulation tests, all of them in an in silico environment.

7 Acknowledgments

O.D.S. thanks National Council of Science and Technology in México (CONACYT) for the scholarship number 263732. G.Q. thanks CONACYT and PAICYT-UANL for financial support under grant numbers 220187 and IT437-15.

8 References

[1] World Health Organization: '*Global report in diabetes*' (France, WHO Press,, 2016)
[2] Tuch, B., Dunlop, M., Proietto, J.: '*Diabetes research*', (CRC Press, London, 2002, 2nd edn)
[3] Femat, R., Ruiz-Velázquez, E., Quiroz, G.: 'Weighting restriction for intravenous insulin delivery on T1DM patient via H_∞ control', *IEEE Trans. Biomed. Eng.*, 2009, **6**, (2), pp. 239–247
[4] Cobelli, C., Dalla Man, C., Sparacino, G., *et al.*: 'Diabetes: Models, Signals, and Control', *IEEE Rev. Biomed. Eng.*, 2009, **2**, pp. 54–96
[5] Harvey, R.A., Wang, Y., Grosman, B., *et al.*: 'Quest for the artificial pancreas: combining technology with treatment', *IEEE Eng. Med. Biol.*, 2010, **29**, (2), pp. 53–62
[6] Gómez, E.J., Hernando, M.E.: 'The INCA system: a further step towards a telemedical artificial pancreas', *IEEE Trans. Inf. Tecnol. Biomed.*, 2008, **12**, (4), pp. 470–479
[7] Chee, F., Fernando, T.: '*Close-loop control of blood glucose*' (Springer, Berlin Heidelberg), vol. **368**
[8] Colmegna, P., Sánchez Peña, R.S.: 'Analysis of three T1DM simulation models for evaluating robust closed-loop controllers', *Comput. Methods Programs Biomed.*, 2014, **113**, (1), pp. 371–382
[9] Bergman, R.N., Ider, Y.Z., Bowden, C.R., *et al.*: 'Quantitative estimation of insulin sensitivity', *Am. J. Physiol.*, 1979, **236**, (6), pp. E667–E677
[10] Hovorka, R., Shojaee-Moradie, F., Carroll, P. V., *et al.*: 'Partitioning glucose distribution/transport, disposal, and endogenous production during IVGTT', *Am. J. Physiol.- Endocrinol Metab.*, 2002, **282**, (5), pp. E992–E1007
[11] Pedersen, M.G., Toffolo, G.M., Cobelli, C.: 'Cellular modeling: insight into oral minimal models of insulin secretion', *Am. J. Physiol. Endocrinol. Metab.*, 2010, **298**, pp. E597–E601
[12] Wilinska, M.E., Hovorka, R.: 'Simulation models for in silico testing of closed-loop glucose controllers in type 1 diabetes', *Drug Discov. Today Dis., Mod.*, 2008, **5**, pp. 289–298
[13] Tiran, J., Galle, K.R., Porte, D.: 'A simulation model of extracellular glucose distribution in the human body', *Ann. Biomed. Eng.*, 1975, **3**, pp. 34–36

[14] Guyton, J.R., O Foster, R., Soeldner, J.S.: 'A model of glucose-insulin homeostasis in man that incorporates the heterogeneous fast pool theory of pancreatic insulin release', *Diabetes*, 1978, **27**, (10), pp. 1027–1042
[15] Sorensen, J.T.: 'A physiology model of glucose metabolism in man and its use to design and asses improved insulin therapies for diabetes', PhD dissertation, Massachusetts Institute of Technology, 1985
[16] Dalla Man, C., Rizza, R., Cobelli, C.: 'Meal simulation model of the glucose-insulin system', *IEEE Trans. Biomed. Eng.*, 2007, **54**, (10), pp. 1740–1749
[17] Dalla Man, C., Micheletto, F., Dayu, L., *et al.*: 'The UVA/PADOVA type 1 diabetes simulator: new features', *J. Diabetes Sci. Technol.*, 2014, **8**, pp. 26–34, https://doi.org/10.1177/1932296813514502
[18] Teodora Chis, O., Banga, J.R., Balsa-Canto, E.: 'Structural identifiability of systems biology models: a critical comparison of methods', *PLoS ONE*, 2011, **6**, (11), e27755
[19] Haidar, A., Wilinska, E.M., Graveston, J.A., *et al.*: 'Stochastic virtual population of subjects with type 1 diabetes for the assessment of closed-loop glucose controllers', *IEEE Trans. Biomed. Eng.*, 2013, **60**, (12), pp. 3524–3533
[20] Visentin, R., Dalla Man, C., Cobelli, C.: 'One-day Bayesian cloning of type 1 diabetes subjects: toward a single-day UVA/Padova type 1 diabetes simulator', *IEEE Trans. Biomed. Eng.*, 2016, **63**, (11), pp. 2416–2424
[21] Prova, B., Ashoke, S., Pallab, D.: 'Estimation of parameters for plasma glucose regulation in type-2 diabetics in presence of meal', *IET Syst. Biol.*, 2018, **12**, pp. 18–25
[22] Kovacs, L., Kulcsar, B., Bokor, J., *et al.*: 'Model-based nonlinear optimal blood glucose control of type I diabetes patients'. 0th Annual Int. Conf. IEEE Engineering in Medicine and Biology Society, Vancouver, BC, 2008, pp. 1607–1610, doi: 10.1109/IEMBS.2008.4649480
[23] Colmegna, P., Sánchez Peña, R.S., Gondhalekar, R.: 'Control-oriented linear parameter-varying model for glucose control in type 1 diabetes'. IEEE Conf. Control Applications (CCA), Buenos Aires, 2016, pp. 410–415, doi: 10.1109/CCA.2016.7587865
[24] Ljung, L.: '*Conventional identification, system identification: theory for the user*' (Prentice Hall, Upper Saddle River, NJ, 1999, 2nd edn)
[25] Ursem, R.K., Vadstrup, P.: 'Parameter identification of induction motors using differential evolution'. Evolutionary Computation, 2003, CEC '03, Canberra, Australia, December, 2003, pp. 790–796, doi:10.1109/CEC.2003.1299748
[26] Zhan, C., Situ, W., Fat Yeung, L., *et al.*: 'A parameter estimation method for biological systems modeled by ODEs/DDEs models using spline approximation and differential evolution algorithm', *IEEE Trans. Comput. Biol. Biomath.*, 2014, **11**, (6), pp. 1066–1076
[27] Dalla Man, C., Raimondo, D.M., Rizza, R.A., *et al.*: 'GIM, simulation software of meal glucose-insulin model', *J. Diabetes Sci. Technol.*, 2007, **1**, pp. 323–330
[28] Rebrin, K, Sheppard, N.F., Steil, G.M.: 'Use of subcutaneous interstitial fluid glucose to estimate blood glucose: revisiting delay and sensor offset', *Biomed. Eng. J. Diabetes Sci. Technol.*, 2010, **4**, (5), pp. 1087–1098
[29] Quiroz, G., Femat, R.: 'On hyperglicemic glucose basal levels in type 1 diabetes mellitus from dynamic analysis', *Math. Biosci.*, 2007, **210**, pp. 554–575
[30] Zhou, K.: '*Essentials of robust control*' (Prentice-Hall, NJ, 1998)
[31] Khalil, H.K.: '*Nonlinear systems*' (Prentice-Hall, NJ, 1996)
[32] Anguelova, M.: '*Nonlinear observability and identifiability: general theory and a case study of a kinetic model for S. cerevisiae*', EngD. dissertation, Chalmers University of technology and Göteborg University, 2004
[33] Ruiz-Velázquez, E., Sánchez, O. D., Quiroz, G., *et al.*: 'Parametric identification of Sorensen model for glucose-insulin-carbohydrates dynamics using evolutive algorithms', *Kymbernetika*, 2018, **54**, pp. 110–1134
[34] Balsa-Canto, E.: 'An iterative identification procedure for dynamic modeling of biochemical networks', *BMC Syst. Biol.*, 2010, **4**, p. 11, https://doi.org/10.1186/1752-0509-4-11
[35] Chis, O., Banga, J.R., Balsa-Canto, E.: 'GenSSI: a software toolbox for structural identifiability analysis of biological models', *IEEE Trans. Comput. Biol. Biomath., Bioinf.*, 2011, **27**, (18), pp. 2610–2611
[36] Torres-Treviño, L.: 'Evonorm: a new evolutionary algorithm to continuous optimization, workshop on optimization by building and using probabilistic models (OBUPM)'. Genetic and Evolutionary Computation Conf., Seattle, Washington, USA, 2006
[37] Eberhart, R.C., Kennedy, J.: 'A new optimizer using particle swarm theory'. Proc. 6th Int. Symp. Micromachine Human Science, Nagoya, Japan, October, 1995, pp. 39–43
[38] Kennedy, J., Eberhart, R.C.: 'Particle swarm optimization'. Proc. IEEE Int. Conf. on Neural Networks, Perth, Australia, 1995, pp. 1942–1948
[39] Lin, H.S., Liauh, W.H., Ho, S.J.: 'OPSO: orthogonal particle swarm optimization and its application to task assignment problems', *IEEE Trans. Syst. Man Cybern.*, 2008, **38**, (2), pp. 288–289
[40] Das, T.K., Venayagamoorthy, G.K., Aliyu, U.O.: 'Bio-inspired algorithms for the design of multiple optimal power system stabilizers: SPPSO and BFA', *IEEE Trans. Ind. Appl.*, 2008, **44**, (5), pp. 1445–1457
[41] Del Valle, Y., Venayagamoorthy, G.K., Mohagheghi, S., *et al.*: 'Particle swarm optimization: basic concepts, variants and applications in power systems', *IEEE Trans. Evol. Comput.*, 2008, **12**, (2), pp. 171–195
[42] Wachowiak, M.P., Smolikova, R., Zheng, Y.: 'An approach to multimodal biomedical image registration utilizing particle swarm optimization multimodal function optimization based on particle swarm optimization', *IEEE Trans. Evol. Comput.*, 2004, **8**, (3), pp. 289–301